Modern Physics Letters B
Vol. 27, No. 13 (2013) 1350093 (10 pages)

DOI: 10.1142/S0217984913500930

SIMULINK MODELING FOR CIRCUIT REPRESENTATION OF GRANULAR CHAINS

LOUIZA SELLAMI
Electrical Engineering Department, US Naval Academy, Annapolis, Maryland, USA
sellami@usna.edu

ROBERT W. NEWCOMB
Department of Electrical and Computer Engineering, University of Maryland, College Park, Maryland 20742, USA
newcomb@eng.umd.edu

SURAJIT SEN
Physics Department, State University of New York, Buffalo, New York 14260, USA
sen@buffalo.edu

Received 27 March 2013
Accepted 28 March 2013
Published 1 April 2013

After a review of the coupled Newton's equations for a small alignment of grains with a fixed reflecting end wall, the equations are put into block diagrams of Simulink. Simulink simulations are given for 6 grain systems for cubic and Hertz intergrain potentials. The expected granular solitary waves are seen in the simulations. The block diagrams hence convert a single impulse into a traveling energy bundle of fixed width. This work forms the necessary first step for the eventual realization of the mathematical system represented by the granular chain as a Very Large Scale Integrated (VLSI) circuit.

Keywords: Grains; Hamiltonian nonlinear system; Hertz potential; solitary waves; Simulink simulation.

PACS Number(s): 05.45.-a, 05.45.Yv, 85.40.-e

1. Introduction

The physical system under consideration comprises a one-dimensional chain of symmetric identical elastic grains in contact with a rigid reflecting wall at one end such that an input pulse travels through compression along the chain. By experiment[1,2] through simulations,[3] and by series approximations,[4,5] the pulses are known to be able to form into solitary waves and since action potentials are solitary waves, these

are similar to the signals used by biological neurons (Ref. 6, p. 42) and of considerable interest for mimicking neural information processing. Therefore, these granular alignments can be seen as an alternate means of forming the pulses used in silicon based pulse coded neural networks.[7] Alternatively, their equations can be put into a form which allows for an equivalent transistor structure having the key properties of the elastic spherical grains. Consequently, with an ultimate goal of mimicking the behavior of the grains in transistor circuits, in this paper we present a Simulink model of these grains in a form that allows for future conversion into VLSI circuits. As is to be seen, the system converts a shock pulse into a non-dispersive bundle of energy that is a solitary wave of fixed width with its velocity dependent on the energy of the shock pulse.

2. Describing Equations

Figure 1 gives a one-dimensional representation of the granular spheres which we here assume all have the same radius R. We consider N grains with q_i being the coordinate of the center of the ith grain. For $i = 1$ an external impulse-like force is assumed applied while for the final grain, at x_N, a rigid wall is assumed. We use the Hamiltonian, $H(p, q)$ representation where p = momentum N-vector and q = position N-vector and H is the sum of the kinetic and the potential, $V(.,.)$, energies. Thus

$$H(p,q) = \sum_{i=1}^{N} \left(\frac{1}{2m} p_i^2 + V(q_{i-1}, q_i) \right) \tag{1a}$$

$$p_i = m \frac{\partial q_i}{\partial t}\,, \tag{1b}$$

$$V(q_{i-1}, q_i) = k[(q_{i-1} + R) - (q_i - R)]_+^{r+1}\,. \tag{1c}$$

Here q_i is the position of the center of the ith grain measured from an origin $q_1 - R = 0$. The potential energy depends on the overlap, $2R - (q_i - q_{i-1})$, of two adjacent grains if positive (and is zero if there is no overlap). As the rest position is $q_{io} = (2i - 1)R$ and the displaced position is $x_i = q_i - q_{io}$ then the overlap is $x_{i-1} - x_i$, which gives the potential energy V if positive with V being zero if there is no overlap; in terms of the x_i, V is seen to be independent of the radius R. So following Ref. 3, the modified symbol $[x]_+ = (x + |x|)/2 = (1 + \text{sign}(x))x/2$ is used in (1) to designate x if $x > 0$ and zero if $x < 0$. The power $r + 1$ is due to the Hertz

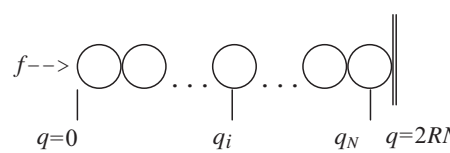

Fig. 1. Chain of grains of equal radii R with a rigid wall placed at the Nth end.

law or any generalization of the same[8,9] and is known to be 5/2 for elastic spheres though we simulate with other r values as well;[9] especially $r = 2$ is convenient for analytic investigations. We set up the equations with r as a parameter which then becomes easy to change in Simulink. The mass of a grain is m and k comprises various constants including Young's modulus.[8,9]

Simulink realizations are most easily obtained through the state variable equations which in this case are the Hamilton differential equations.

$$\frac{\partial q_i}{\partial t} = \frac{\partial H}{\partial p_i} = \frac{1}{m} p_i \,, \tag{2a}$$

$$\frac{\partial p_i}{\partial t} = -\frac{\partial H}{\partial q_i} = m \frac{\partial^2 q_i}{\partial t^2} \,. \tag{2b}$$

By the choice of $x_i = q_i - q_{io}$ and $z_i = p_i/m$, and introducing possible loss (by the parameter k_{loss}) we recast these into the following state-variable form which are the actual ones we put into Simulink in the following paragraphs.

$$\frac{dx_i}{dt} = z_i \,, \tag{3a}$$

$$\begin{aligned} \frac{dz_i}{dt} &= \frac{d(\frac{dx_i}{dt})}{dt} \\ &= \left(\frac{k(r+1)}{2^r m}\right)\{((1+\text{sign}(x_{i-1}-x_i))(x_{i-1}-x_i))^r \\ &\quad - ((1+\text{sign}(x_i - x_{i+1}))(x_i - x_{i+1}))^r\} - k_{\text{loss}} z_i \,. \end{aligned} \tag{3b}$$

Equations (3) are for $i = 2, \ldots, N$ while at $i = 1$ an additive input term, $f(t)$, is to be added and the x term omitted fixing the input end boundary, via $x = 0$, while for the Nth grain a fixed boundary is imposed by fixing $x_{N+1} = 0$, for $q_{N+1} = (2N+1)R$. The factor $k' = k(r+1)/(2^r m)$ can be considered a scale factor on time in which case it will be normalized to 1, though we allow other values in the Simulink blocks. Note also that the x_i are distances so measured in meters and that due to the differencing the actual radius R cancels out of Eq. (3). For solitary waves of velocity c, we have $x_i(t) = u(x_i - ct)$. Following normalizations of Chatterjee,[3] this gives the second order differential equation for the solitary wave

$$\ddot{u} = [u(t+1) - u(t)]_+^r - [u(t) - u(t-1)]_+^r \,. \tag{4}$$

Nesterenko[1] solved this equation using a long wavelength approximation and by drawing parallels between this problem and the Korteweg–deVries problem.[10] From these, Chatterjee[3] shows MatLab simulations indicating the existence of solitary waves while Sen and Manciu[4] give a series solution approximation. In detail,[5] with $\alpha = x_i - ct$ and n a parameter.

$$u(\alpha, n)) = \frac{A}{2}(1 - \tanh(F(\alpha(n))) \tag{5a}$$

$$F(\alpha, n)) = \frac{1}{2}\sum_{q=0}^{\infty} C_{2q+1}(n)\alpha^{2q+1}\,. \tag{5b}$$

The C_{2q+1} have been evaluated for $q = 0, \ldots, 5$ and the results shown to be solitary type waves (see Fig. 3.1 of Ref. 5). In short, these grains are known to support solitary waves.

Consequently, we know that we can obtain solitary waves from the state variable equations (3) so it is to them we turn for possible transistor realization. Toward that we obtain next a suitable block diagram realization.

3. Simulink Block Diagrams

In the following, we explain in some detail the basic functioning of the block diagrams. Although we have simulated for much larger N, for convenience of illustrating details, the top of Fig. 2 shows a Simulink block diagram for $N = 6$ stages of grains. The very left square is a Simulink block for the pulse used as the force input and to the right of it are four blocks of constants and another one for adding the input pulse with any possible feedback via the lower right triangle gain block (which is set to 0 in the absence of feedback for this paper). At the very bottom are two Simulink scope blocks, the left one for display of the velocity of grains 2 and 5 and the right one for displacement of the same two grains (the heavy vertical lines feeding the scopes are multiplexer blocks which allow the simultaneous display of two signals). The left most large rectangle represents the input grain and has seven inputs as labeled (on the left) and one output (the position) on the right. The right most large rectangle represents the end grain, again with seven inputs and one used output. The middle square represents four grains and is expanded in the bottom of Fig. 2 into four sub-blocks, for grains numbered $i = 2, 3, 4, 5$ with each having internal structure being given in detail by Fig. 3. In Fig. 3, the rounded rectangles (numbered 1–6 with labels such as $\ln r$) represent input terminals for constants and positions of the grains to the left and the right; the other two rounded rectangles represent the grain's position and velocity as outputs of the Simulink block for the grain. The 1/s square blocks on the lower right are integrator blocks for taking the integrals of Eq. (3), with IC denoting initial conditions. The circles are blocks which perform addition and subtraction and the $|u|$ block takes the absolute value, as used for $\{\cdot\}+$ as mentioned in the text below Eq. (1c). The two square blocks in the upper middle raise u to the power v. u is the signal on the top input lead and comes from the amplifier of gain 0.5. These blocks are used to raise the signal in the top left lead to the power r where r comes from the input labeled $\ln r$ [see Eq. (3b)]. This allows us to observe the velocity, v_i, as well as the displacement x_i. We have also allowed for the choice of actual position, q, by input of grain radii but choose $R = 0$ when x is taken as displacement around equilibrium, that is, the choice of x_i as being equal to q_i results when nonzero R is inserted in these blocks. Using the same Simulink components the input, $i = 1$, and output, $i = N$,

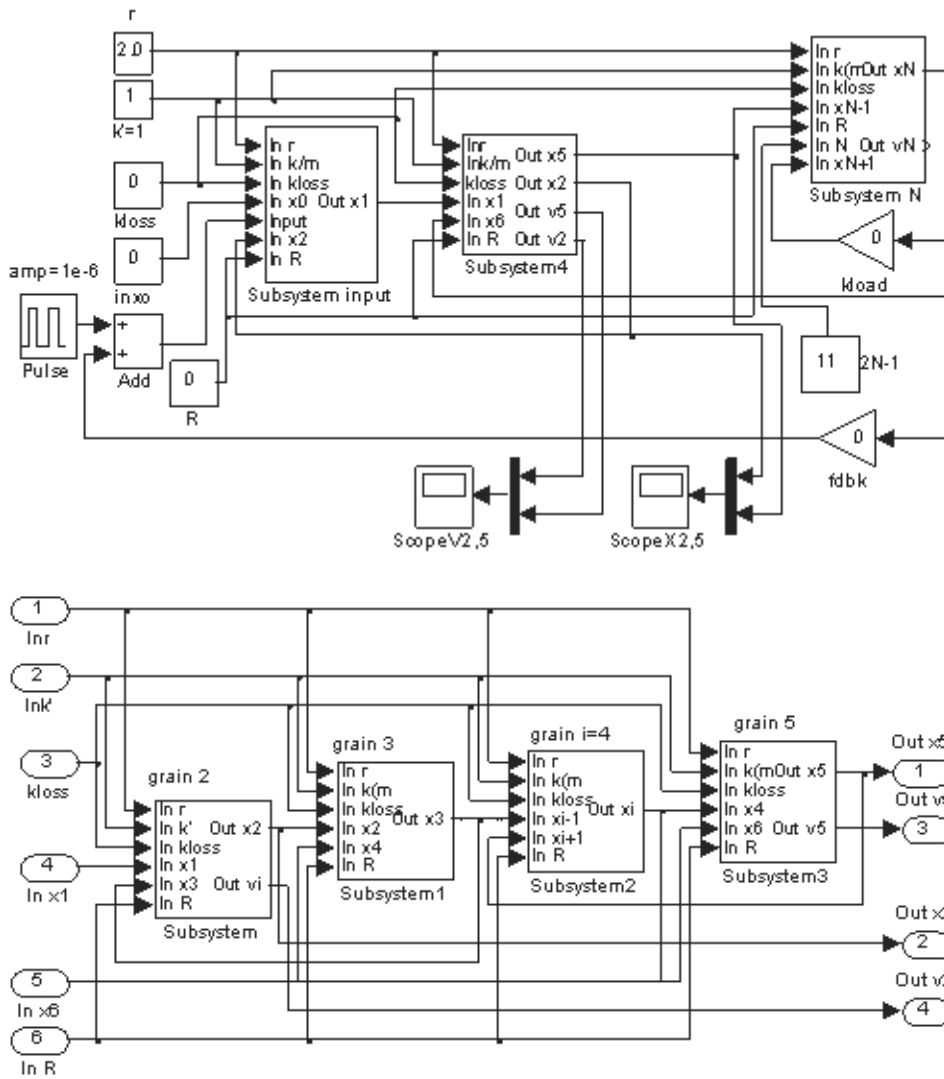

Fig. 2. Simulink 6 grains block connection (top) with Subsystem 4 expanded (bottom).

stages are expanded as shown in Figs. 4 and 5. Figure 3 realizes Eq. (3) while the input and output stages, are simple modifications reflecting their different loading. In Fig. 2 an input pulse of amplitude 10^{-6} is applied for normalized $t = 0.05$, on the left to the input stage. As seen in Fig. 3, different initial conditions can be set in the integrators, though the presented runs are for all IC $= 0$. And as seen in Fig. 2, the velocities are multiplexed so that two of them can be observed simultaneously on the one scope (to also be read into Matlab via the Simplot (scope#) command for editing).

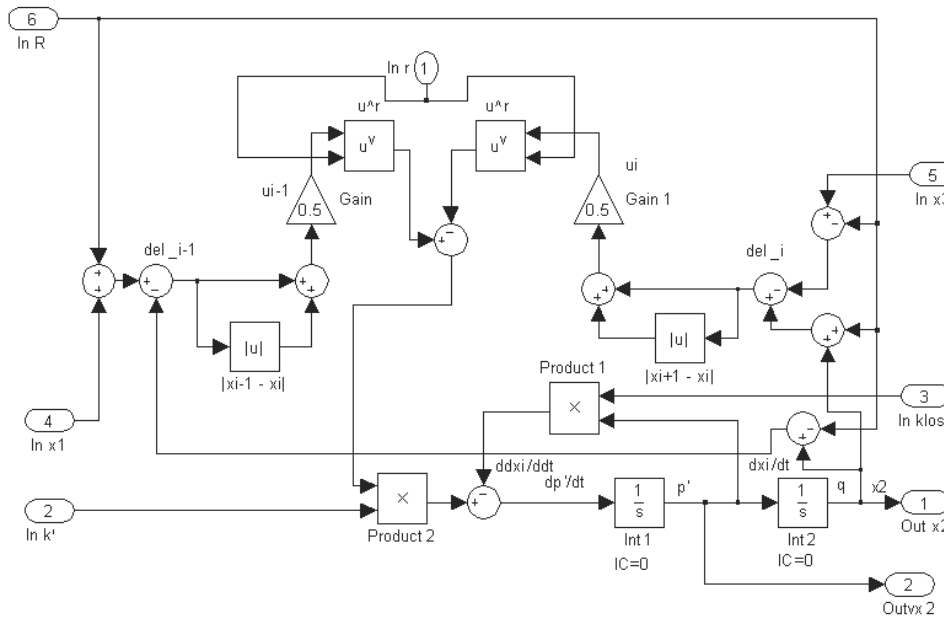

Fig. 3. Simulink ith internal grain stage, $i = 2$.

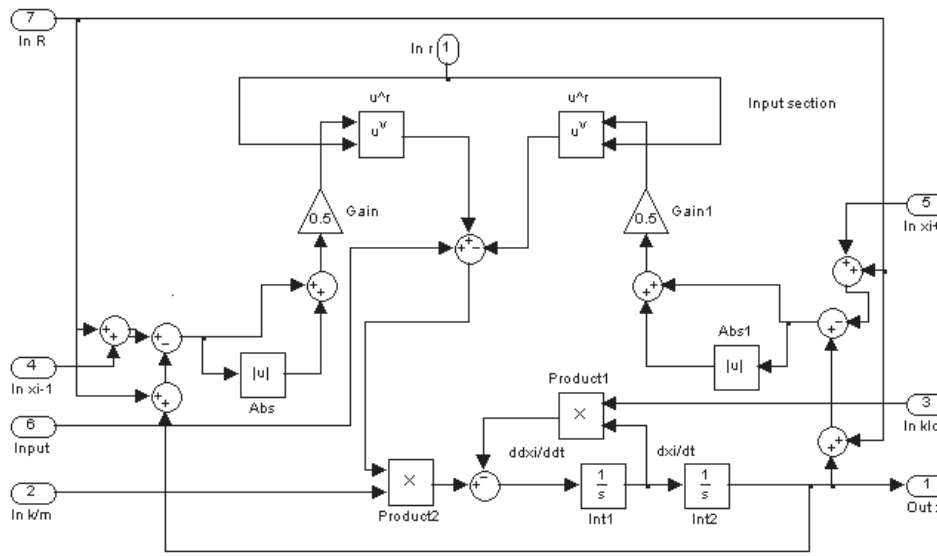

Fig. 4. Detailed Simulink input grain stage, $i = 1$.

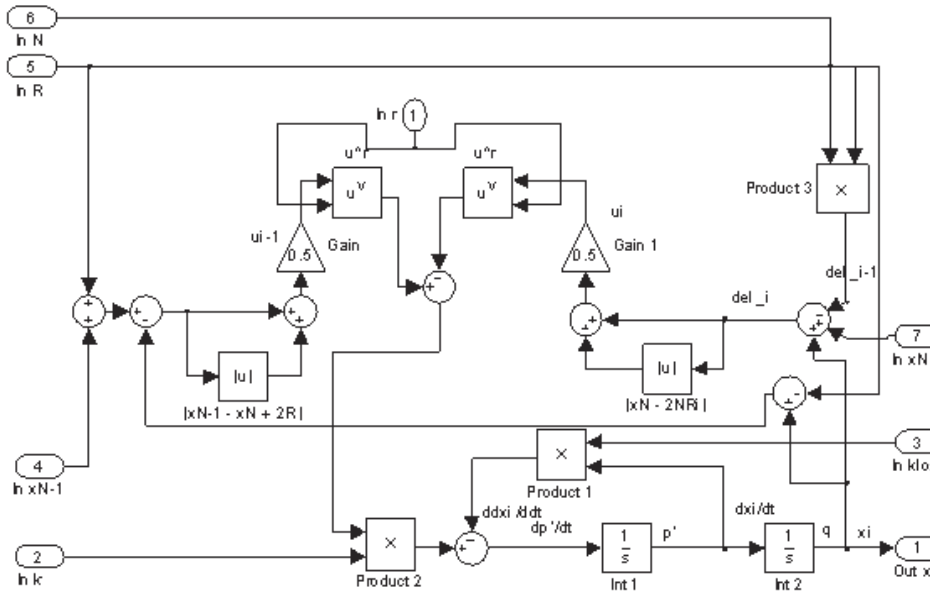

Fig. 5. Detailed Simulink output grain stage, $i = N$.

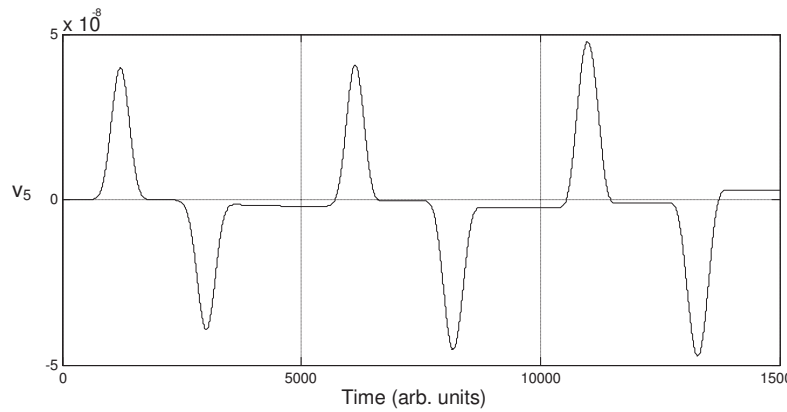

Fig. 6. Simulation results of velocity dx/dt for $r = 2$ at 5th grain for $N = 6$ for a 15,000 time run, y axis in meters/normalized seconds.

4. Simulation Results

Figure 6 gives a plot of dx/dt at the fifth stage for $r = 2$ and k' factor normalized to 1, showing solitary waves as well as their reflection from the $N = 6$ end wall. For more details, in the top panel of Fig. 7 are shown the displacement around equilibrium for the 2nd and 5th grains while in the bottom panel are the velocities of those grains. For Figs. 6 and 7, the square input pulse is of amplitude 10^{-6} and

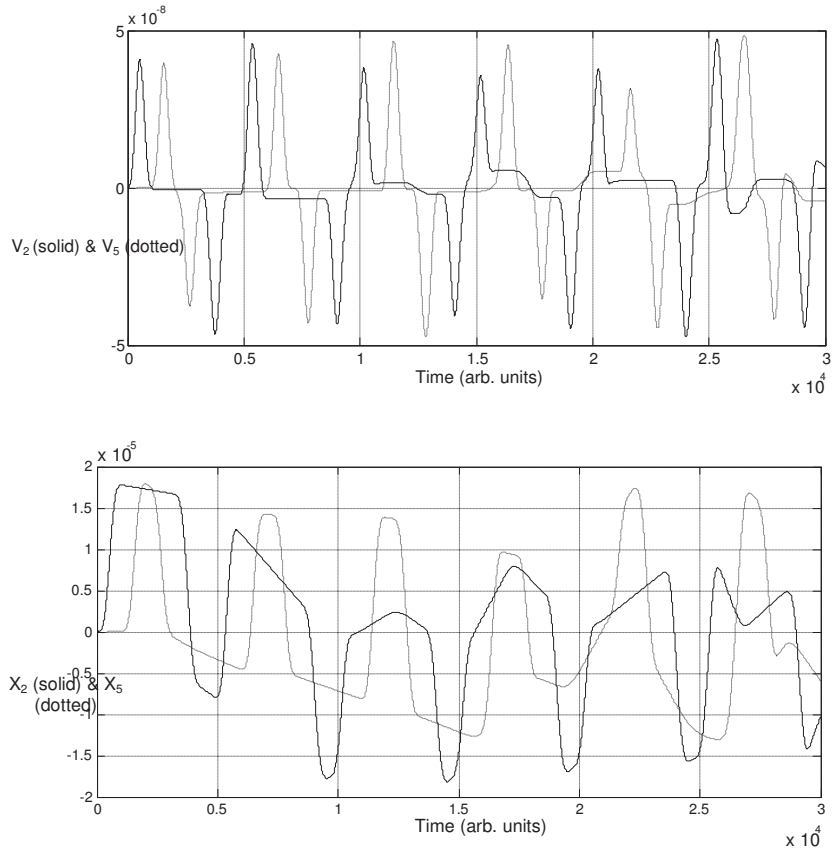

Fig. 7. Velocity (top panel) and displacement (bottom panel) curves comparing 2nd and 5th stage signals for a 30,000 time run.

pulse width $t = 0.05$. This results in a delayed traveling velocity wave to within the accuracy of Matlab. A reflected wave can be seen via the negative velocity signal. A similar situation is shown for the Hertz, $r = 1.5$, case in Fig. 8 where it is seen that the signals are sped up over the square law, $r = 2$, case. In both cases, numerical instabilities appear to result, being earlier for smaller r. In these simulations the ODE45 equation solver of Simulink was used. If other than zero R is chosen, the x_i become the q_i and the latter increase around $2iR$ so we find the use of x_i as displacement around equilibrium to be more convenient and numerically more stable than using q_i. We have also added up to 51 grains but find that the numerical error becomes a problem when running Matlab, as pointed out by Chatterjee.[3]

5. Discussion

For obtaining Simulink models we have put the grains differential equations into state variable form, in (3) above. From these we are able to set up block diagrams

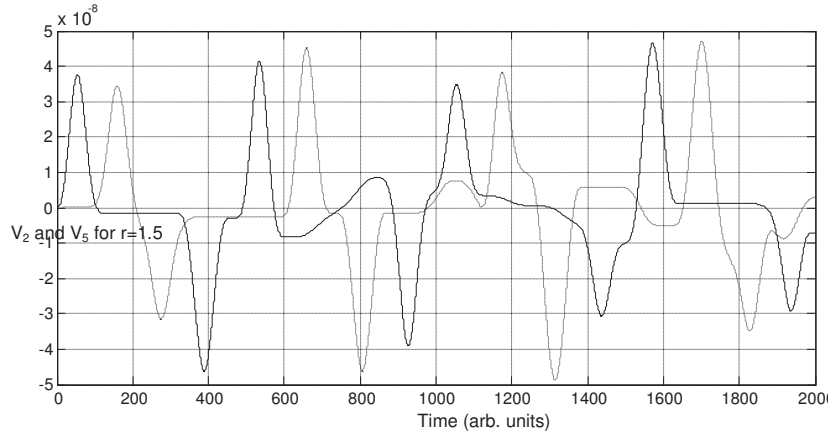

Fig. 8. Results for $r = 3/2$, for velocities of 2nd (solid line) and 5th (dotted line) grains for a 2,000 time run.

which use only integrators, multipliers, powers (including square roots), and summers. These are conveniently put into Simulink through which we have again shown that solitary types of signals can be observed in the grain velocities. In the case of grains satisfying the Hertz potentials these blocks necessitate square roots in obtaining the 3/2 power. However, from the simulations we obtain similar results for powers of $r = 2$ as well as 3/2, though with a different time scaling as for example the 4th stage peak occurs at $t = 200$ for $r = 3/2$. We have normalized to $k' = 1$ and considered x_i as the displacement around equilibrium, but we can consider it alternatively as the absolute center position, q_i, of the ith grain for which the value of the radius R is needed (with $R = 0$ chosen for the right wall). If we choose to work with the q_i the positions increase with i and become less accurate numerically. In the Simulink system we do have the capability of choosing different R's for the different grains as well as using any real r along with the added possibility of including loss, though it is not present in the basic grains equations or in the simulations presented. By fixing the boundaries, via $x = x_{N+1} = 0$ the grains can bounce back and forth as clearly seen in the simulations.

The above can be generalized to also allow for different materials of different individual grains within the system, these being allowed for by separate ports in the individual grain cell blocks.

It should be noted that one of the difficulties in working with these grains is that the potential energy of a grain loses a term when there is separation from an adjacent grain, this being handled by the use of the $[\cdot]_+$ terms in the equations, and these being handled by the middle portions seen in Figs. 3–5.

Some useful additional references are included (Refs. 11–21). For example, there are other effects which can be included, one of which uses the "coefficient of restitution",[12] while generalization to higher dimensions is possible, such as for

sand at the beach. Also the above equations are normalized though denormalization is easily carried out. (Ref. 21 gives material constants for various materials.)

Since the state-variable equations (3) are readily realizable by transistor circuits, these granular chain systems are also amenable to VLSI fabrications. For that the Simulink blocks have been set up in a form suitable for realization by integrated CMOS transistor circuits. In that case the choice of $r = 2$ is most convenient since it can be realized by squaring circuits. And due to the absolute value in Eq. (3b) the squaring circuits need only be two quadrant, rather than four quadrant, ones. Also the presented results are for lossless grains while in actual ones there would be dissipation; certainly transistor circuits can realize lossless, as well as lossy systems, since they take bias power to compensate for loss. Nevertheless, we have included in the Simulink blocks provision for inclusion of loss.

Acknowledgments

The authors wish to acknowledge Professor Krishna Shenai of the University of Toledo for bringing them together on this problem. S. Sen acknowledges support of an US Army Research Office — STIR grant.

References

1. V. F. Nesterenko, *J. Appl. Mech. Tech. Phys.* **24** (1983) 733.
2. C. Coste, E. Falcon and S. Fauve, *Phys. Rev. E* **56** (1997) 6104.
3. A. Chatterjee, *Phys. Rev. E* **59** (1999) 5912.
4. S. Sen, M. Manciu and J. D. Wright, *Phys. Rev. E* **57** (1998) 2386.
5. S. Sen and M. Manciu, *Phys. Rev. E* **64** (2001) 056605.
6. W. F. Ganong, *Review of Medical Physiology* (Lange Medical Pubs., Los Altos, CA, 1985).
7. M. E. Zaghloul, J. L. Meador and R. W. Newcomb, *Silicon Implementation of Pulse Coded Neural Networks* (Kluwer, Boston, 1994).
8. H. Hertz, *J. Reine Angew. Math.* **92** (1881) 156.
9. D. Sun, C. Daraio and S. Sen, *Phys. Rev. E* **83** (2011) 066605.
10. D. J. Korteweg and G. de Vries, *Phil. Mag.* **39** (1895) 422.
11. S. Sen, J. Hong, J. Bang, E. Avalos and R. Doney, *Phys. Rept.* **462** (2008) 21.
12. G. Kuwabara and K. Kono, *Jpn. J. Appl. Phys.* **26** (1987) 1230.
13. S. Job, F. Melo, A. Sokolow and S. Sen, *Phys. Rev. Lett.* **94** (2005) 178002.
14. S. Sen and M. Manciu, *Physica A* **268** (1999) 644.
15. M. Manciu, S. Sen and A. J. Hurd, *Physica D* **157** (2001) 226.
16. E. Falcon, B. Castaing and M. Creyssels, *Eur. Phys. J. B* **38** (2004) 475.
17. F. Hermann and P. Schmaeizle, *Am. J. Phys.* **49** (1981) 761.
18. F. Herrmann and M. Seitz, *Am. J. Phys.* **50** (1982) 977.
19. R. P. Simion, *Nonlinear Granular Breathing*, Doctoral dissertation, Department of Physics, State University of New York at Buffalo, May 2010.
20. V. F. Nesterenko, *Dynamics of Heterogeneous Materials* (Springer, New York, 2001).
21. J. Yang, C. Silvestro, D. Khatri, L. De Nardo and C. Daraio, *Phys. Rev. E* **83** (2011) 045505.